Journal of Computational Applied Mechanics 2025, 56(4 ): 863-881

DOI: 10.22059/jcamech.2025.388538.1333

RESEARCH PAPER

# Effects of substrate stiffness and anti-cancer drug on morphology and viability of Prostate cancer cell lines

Sayed Reza Ramezani [a], Afsaneh Mojra [a *], Mohammad Tafazzoli-Shadpour [b]

[a] *Department of Mechanical Engineering, K. N. Toosi University of Technology, Tehran, Iran*
[b] *Faculty of Biomedical Engineering, Amirkabir University of Technology, Tehran, Iran*

**Abstract**

**Cancer cell detection in various tissues of the body, as well as during chemical medication treatment, can aid in identifying these cells and providing faster and more effective treatments. Studies have been conducted to aid in the diagnosis and identification of cancer cells. Although significant progress has been made, there is still a need for research in this sector, particularly when multiple variables are considered at the same time. The present study has the novelty of examining the simultaneous effects of cell culture substrates and chemical drugs on the morphology of two cancer cell lines with different degrees of invasion. In the current study, two cell lines with varying degrees of metastasis were cultivated on three surfaces with varying elastic modulus, and their morphology was studied using photography and image processing with code and software. In this study, the cell morphology was evaluated with great precision. In addition, the cell viability of these two cell lines was assessed for the aforementioned groups in order to determine the rate of cell death in each group. The findings show that drugs have a greater impact on cell morphology than substrates and cell types, and that the two cell lines respond differently to drug and substrate combinations, with DU145 cells being more susceptible to drug-induced cytotoxic effects. primarily on soft substrates. Understanding these interactions is critical for adapting treatments to the specific properties of prostate cancer cells, which could improve outcomes for patients with various metastatic tendencies.**

**Keywords:** cell morphology, Prostate cell lines, substrate stiffness, Extracellular matrix; Anticancer drugs;

## 1. Main text

## 1. Introduction

The physical and anatomical characteristics of cellular elements have become critical markers of physiological and pathological occurrences [1-3]. Specifically, the actin cytoskeleton and its regulatory proteins are essential for several aspects of cancer metastasis, particularly for invasion and migration [4, 5]. During these dynamic processes, the actin cytoskeleton—which is located beneath the cell membrane as a scaffolding network—undergoes complex remodelling that produces intrinsic forces that are essential for cell invasion, migration, and spreading. As a result, measuring morphological alterations and cytoskeleton reorganization offers a valuable method for early cancer identification. Moreover, studying morphological characteristics advances our understanding of the physical mechanisms and underlying processes that control the spread of cancer. The complex way that prostate cancer cells

react to their surroundings is one of the many features of prostate cancer development that are yet unclear [6-8]. The creation of an in vitro model for cell growth and differentiation is critical to understanding basic mechanobiology and its possible medical uses in organ replacement after injury. Numerous materials have been investigated to see how they affect cell behaviour in the context of cell culture [9-13]. These materials permit the development of microfluidic organ-on-a-chip culturing systems. These materials make it easier to create microfluidic organ-on-a-chip culturing systems, which successfully imitate the functional unit of an in vitro human living organ while offering an environment favourable to cell viability. The regulation of cellular activity, including factors like cell shape, proliferation, and differentiation, is greatly influenced by the extracellular matrix (ECM). These processes can be significantly altered by changes to the chemical composition and mechanical characteristics of the ECM [14]. Notably, rheumatoid arthritis and chronic kidney diseases are among the many chronic illnesses that are known to exhibit ECM degradation, which is linked to impaired tissue integrity [15]. Because they replicate in vivo conditions, artificial ECM systems are helpful in studying the interactions and regulation of cellular processes and tissue integrity in healthy and pathological conditions [16]. Also, biomedical research frequently uses both natural biomaterials like collagen and gelatin as well as synthetic materials like polyacrylamide (PAAm) gel and polydimethylsiloxane (PDMS) [17-19]. One significant benefit of PAAm gels is that their stiffness may be adjusted from 0.3 to 300 kPa [20]. A more in-depth investigation of the interaction between cellular responses and the mechanical characteristics of the scaffold is made possible by this flexibility in stiffness [21]. Nevertheless, PAAm gels need help with simulating the ECM in nature. First, because the ECM is a dynamic system rather than just an inert scaffold, its ability to interact with the physiological environment is limited. Second, there may be a cytotoxicity risk due to unreacted acrylamide residues in the PAAm network. It is possible to address these issues by using hydrolyzed PAAm hydrogels. These viscoelastic polymeric networks, which have a hydrophilic topology, get around the drawbacks of conventional PAAm gels [22, 23]. Hydrolyzed PAAm hydrogels are biocompatible polyelectrolytes that can absorb, hold, and release large amounts of biological fluids when needed. These hydrogels are widely used in investigations on cell connection, artificial muscle formation, and drug administration. They offer adaptable solutions for various biomedical applications [24-26].

The substrate stiffness in which cancer cells sense and respond before and after treatment has not been thoroughly studied despite a plethora of studies investigating the effects of substrate stiffness on cellular activities. Due to metastasis, cancer cells go to different tissues, and there they sense different elastic modulus of ECMs. In the present study, to model ECMs with different elastic modulus, PAAm substrates with different elastic modulus were used as a substrate for cell culture. Figure 1 shows a schematic of the present study's process. In the present study, the morphology of two cell lines with different levels of invasion on substrates with three different elastic modulus and for two groups of cells treated with chemical drugs and untreated cells has been investigated by photographing with a microscope and processing the images with a code based on color contrast. Also, the cell viability of these two cell lines has been checked on substrates with three different elastic modulus and for two groups of cells treated with chemical drugs and untreated cells, so that the results of morphology and cell viability can be observed simultaneously. The results of the present study can assist future studies in detecting and identifying cancer cells in various tissues.

## 2. Material and methods

Two types of prostate cancer cell lines with different degrees of metastasis (higher metastatic potential (DU145) compared to LNCAP cells, which have low metastatic potential) were cultured on three substrates with different elastic modulus (soft, medium, and stiff) and were treated with Abiraterone Acetate drug. Cell morphology was divided into four different groups. Also, the cell viability (live/dead) assay was performed in the treated group with Abiraterone Acetate drug and control group on three substrates with different stiffness.

### *2.1 Manufacturing and preparation of acrylamide substrates*

The preparation of polyacrylamide gels entails the formation of aqueous solutions containing Acrylamide monomer (AAm) and N, N′-Methylene bis acrylamide (cross-linker, Bis-acrylamide) at concentrations of 40% and 2% weight/volume, respectively. Subsequently, varying quantities of Bis-acrylamide and AAm were formulated in deionized water (DW). To initiate the free radical polymerization reaction, it was necessary to use Ammonium Persulfate (APS) at a concentration of 10% weight/volume, which was activated by N, N, N′, N′-Tetramethyl ethylenediamine (TEMED) at a purity of 99%. Diverse polyacrylamide gels were generated by employing varying degrees of cross-linking density. The gels were prepared by combining different concentrations of AAm, DW, APS, and TEMED, as specified in Table 1. Following a comprehensive blending procedure, the gel solution was transferred into a rectangle glass slide, positioned between two more glass slides, and allowed to undergo polymerization for a duration of 3 hours at ambient temperature. Once the polymerization process was completed,

the layers of Polyacrylamide (PAAm) gel were cautiously extracted from the mold and immersed in a 1 M sodium hydroxide (NaOH) solution for the entire night. This caused a hydrolytic transformation of the PAAm gel to take place.

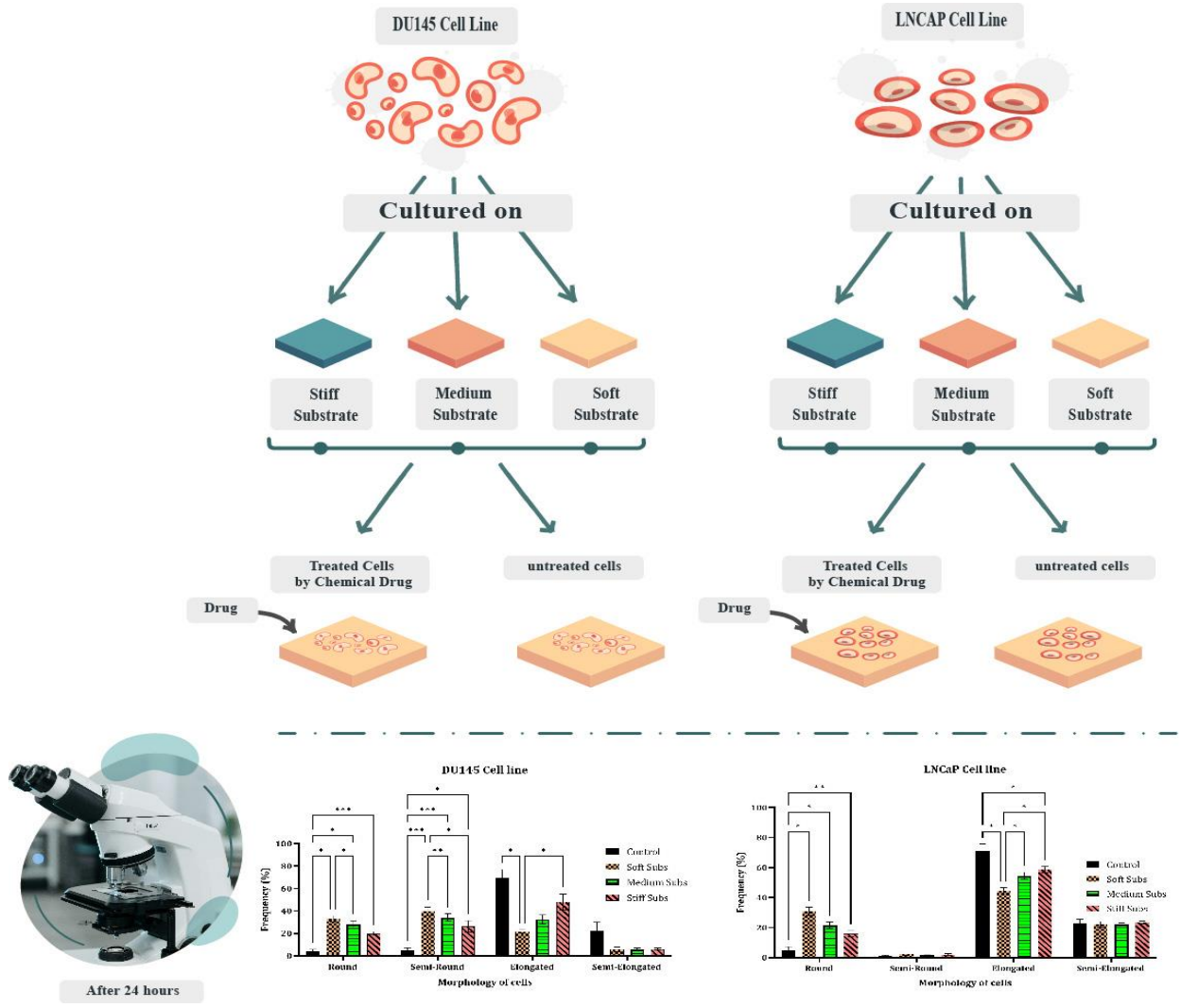


**Fig. 1- Two prostate cancer cell lines were cultured on three substrates with different elastic modulus and cell morphology and cell viability were examined for the groups of cells treated with chemical drugs and untreated cells.**

*2.2 Young's modulus measurement of substrates*

The samples were subjected to tensile testing in order to determine the elastic modulus. The samples were fabricated and evaluated in a cylindrical mold with dimensions of 1 inch in diameter and 1 inch in height. Each specimen underwent three repetitions, and a total of nine specimens were tested in accordance with ASTM criteria. The tensile testing was performed in accordance with precise criteria, employing a strain rate of 20 mm per minute and a load of 10 N. Fig. 2 illustrates the tensile tests performed on the substrates.

Figure 3(A) to (C) depicts the stress-strain diagram for a sample taken from each substrate group. The slop of the line in the elastic region of the graphs represents the elastic modulus and is highly associated with the stiffness of the substrate. Soft and medium samples exhibit less steep gradients compared to stiff samples, suggesting a higher ability to undergo deformation under the same external load. Additionally, the data unambiguously demonstrates that stiff samples undergo fracture when they reach a strain of approximately 0.5, but more flexible samples (soft and medium substrates) do not experience fracture. The stress-strain diagram of the sample displays clearly defined loading and unloading phases. Figure 3(D) displays the elastic modulus of all the samples.

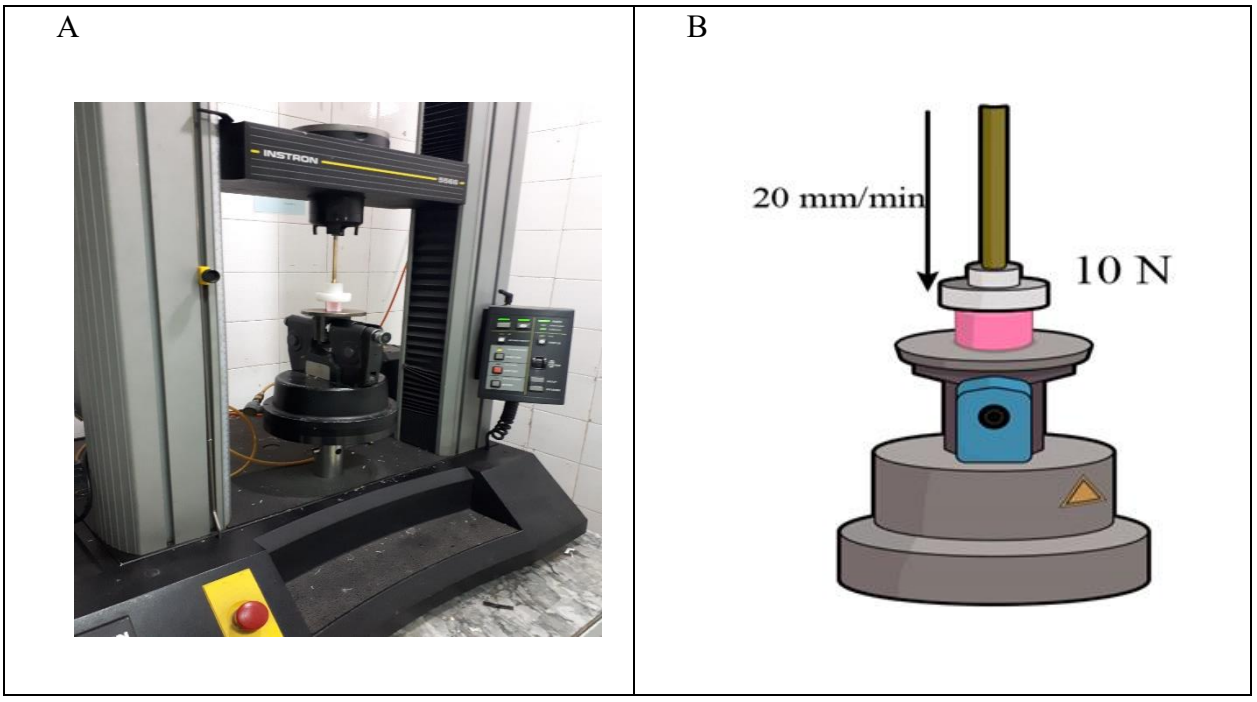


**Fig. 2- The substrates underwent tensile testing using cylindrical molds with a diameter and height of 1 inch. The samples were subjected to a strain rate of 20 mm per minute and a load of 10 N. Each elastic modulus was measured using three samples. (A) Actual image of sample in test mode and (B) Animated image.**

*2.3 Fibronectin coating and cell seeding*

Fibronectin is a type of protein. This product is optimal for the application of a thin coating on cell culture surfaces, hence improving cell adherence and proliferation in vitro. Also, these cause more accurate simulation in vivo and in vitro. The surface was coated with a concentration of $2\frac{\mu g}{mliter}$ of fibronectin and incubated at a temperature of $37°C$ for one hour to induce changes. Following the removal of surplus fibronectin, the cells were cultivated at a density of $10^4\ cell/_{cm^2}$. Afterward, the substrates were delicately rinsed with phosphate-buffered saline (PBS) in order to eliminate any surplus fibronectin, thereby guaranteeing a consistent coating. Following the application of fibronectin coating onto the substrates, the substrates were prepared for cell seeding.

*2.4 Cell culture*

DU145 and LNCaP cell lines were purchased from the Iranian Biological Resource Center. Cell lines were cultured with DMEM (Gibco, USA) and 10% FBS (Gibco, USA). Cells were passaged when they reached 80% confluence. These cells were used in the tests of this study.

*2.5 Drug solution preparation*

The anti-cancer drug Abiraterone Acetate was sourced in powder from the Sobhan Oncology, Iran for this study. The IC50 of this medication was obtained using the MTT assay, as described in the preceding section. The medication powder was carefully and precisely concentrated using DMSO solutions. The fluid underwent filtration using a 0.22-micron filter. Prior to application, the drugs underwent further dilution with culture media at a ratio of 1:1000. The medicine was administered to cell groups for a duration of 24 hours during each iteration of the experiment.

*2.6 Metabolic activity (MTT assay)*

The toxicity level of Abiraterone Acetate drug on cell lines was checked by MTT test. At first, $10^5$ cells were seeded in a 96-well microplate. After 24 hours, cells were treated with different concentrations of the drug (7.8125, 15.625, 31.25, 62.5, 125, 250 and 500 µM). Cells were exposed to 0.5 mg/ml MTT for 4 hours, and then 150 µl DMSO was added to each well. Eliza Reeder read the optical absorbance of each well at 570 nm. The software GraphPad Prism (version 10.10) was utilized to create dose-response curves through the implementation of nonlinear regression analysis and Chou-Talalay method was used.

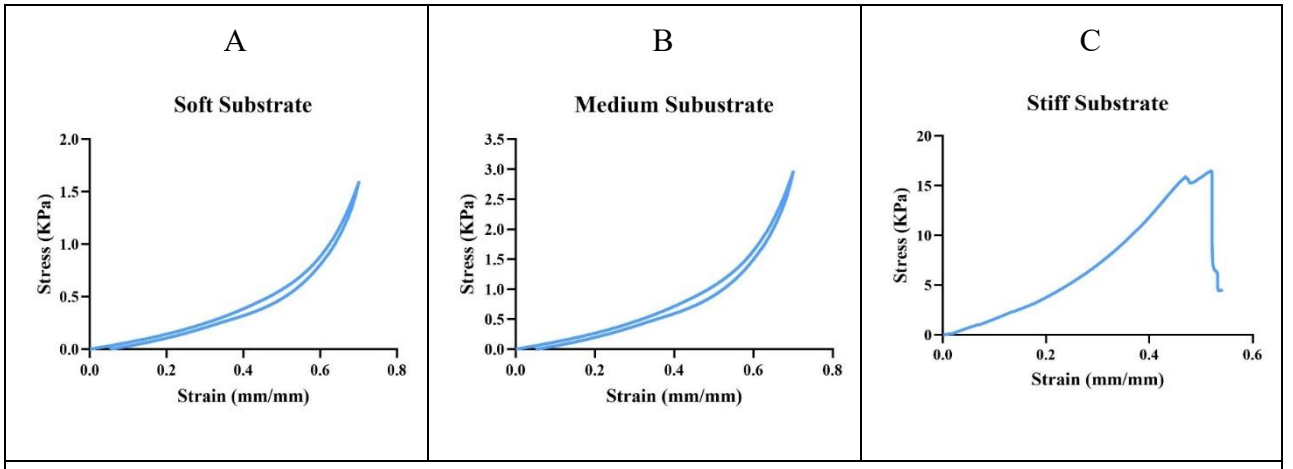


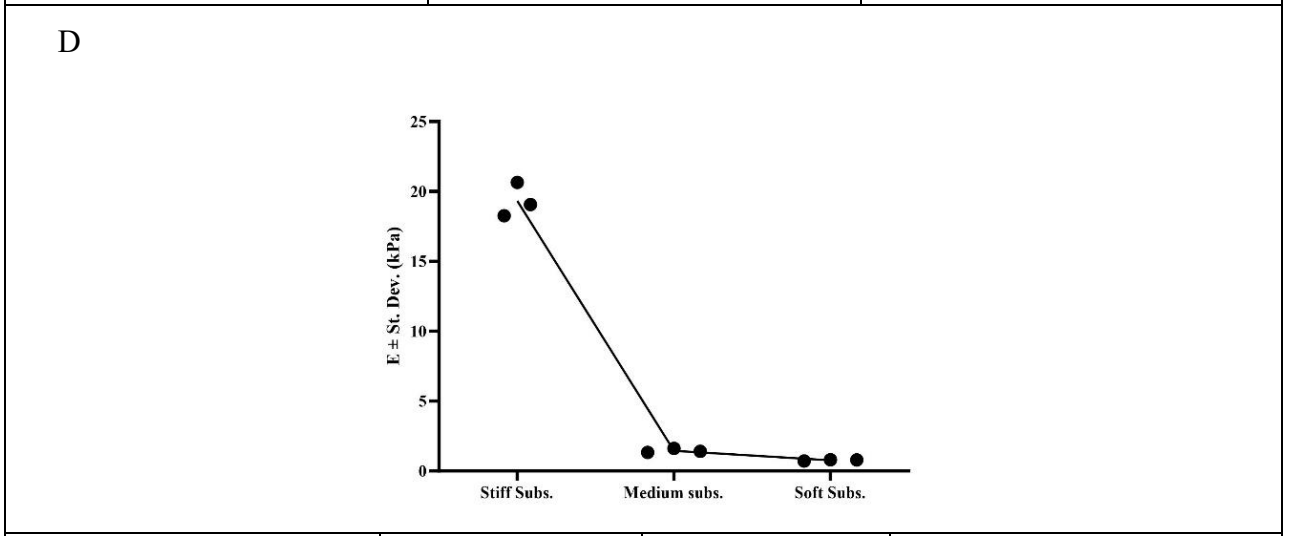


| | Stiff substrate | Medium substrate | Soft substrate |
|---|---|---|---|
| **Modulus of Elasticity** | $19.325 \pm 1.3278$ | $1.449 \pm 0.1634$ | $0.7703 \pm 0.058$ |

**Fig. 3- The stress-strain diagrams are provided for each substrate group, including the (A) soft substrate, (B) medium substrate, and (C) stiff substrate. (D) The calculated value of the modulus of elasticity, which was repeated three times for each group.**

*2.7 cell viability (live/dead) assay*

To characterize the rate of live cells, a fluorescence-based kit was used according to the manufacturer's protocol after 24 hours of treatment. In short, an orange solution (Sigma 9231A) is applied to the cells for 15 minutes at room temperature. After that, they are rinsed three times with PBS (4417P-Sigma). Then, PI (4864P-Sigma) is introduced to the cells and rinsed three times with PBS. A fluorescent microscope (Olympus IX70) is used to capture images. Observation of cells, both living and deceased, is possible within 30 minutes. The cell viability percentage was determined by tallying the number of green points, which indicate live cells, and then dividing it by the total number of cells.

## 3. Results

After the materials were described in the previous section, this section presents the results of the assays. The current investigation involved culturing two cell lines (DU145 and LNCAP) on three different substrates (stiff, medium, and soft stiffness). For each substrate, experiments were conducted on two groups: one group was untreated, while the other group was treated with Abiraterone Acetate, unless otherwise stated. Initially, the IC50 of

the medication was determined for both cell lines, 24 hours after the treatment. These concentrations were subsequently utilized for the assays. Next, the morphology of both the untreated and treated cell groups was analyzed. In addition, the cell viability of the specified groups was assessed.

*3.1 Treatment assessment by MTT assay*

A study was conducted using an MTT assay on soft substrates to evaluate the impact of drugs on cells. The IC50 of Abiraterone Acetate drug on cell lines (DU145 and LNCaP) was determined, and the same concentrations were applied for subsequent tests. Cell viability of treated cells was compared to untreated cells (control group) and plotted against drug concentration on a logarithmic scale. Chou-Talalay method [27, 28] was employed to assess the IC50 of the DOC, Abir. The drug in DU145 and LNCaP cell lines.

Fig. 4 indicates the toxic effect of Abiraterone Acetate in two cell lines, DU145 (Fig. 4A) and LNCaP (Fig. 4B). The graph of cell viability based on the logarithm of Abiraterone Acetate drug concentration shows that with increasing drug concentration, the toxicity of the drug on cancer cells increases, and the cell viability rate decreases. IC50 of the drug for the DU145 cell line was 110.9µM, and for the LNCaP cell line was 328.3uM. This result shows that the toxic effect of the drug on the DU145 cell line was more than the LNCaP cell line.

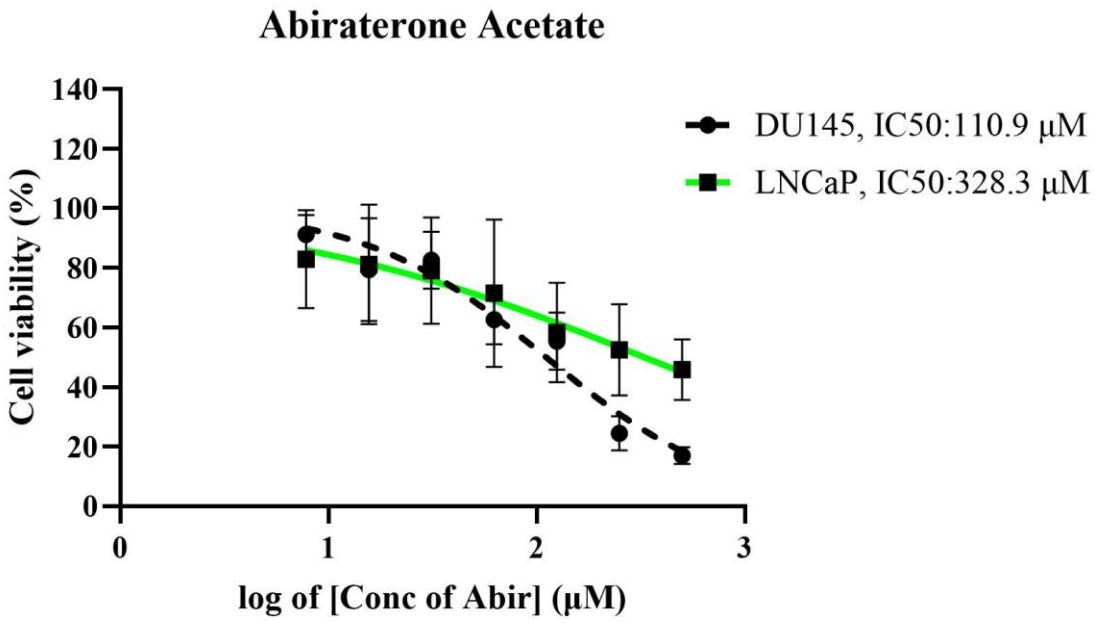


**Fig.4: Dose-response curves are calculated using the logarithm of Abiraterone Acetate concentrations on DU145 and LNCaP cell lines. Calculation of IC50 was done with Graph Pad Prism 10.2.3. 24 hours after treating the cells with the drug at different concentrations, the MTT assay was performed on the cells to obtain the IC50 concentration for treated cell lines.**

*3.2 Effect of substrate and drug on Cell circularity morphology*

After the IC50 concentration of Abiraterone Acetate drug on two cell lines was calculated in the previous section, in this section we want to investigate the morphology of two cell lines with different invasion on three substrates with different stiffness and in treated and untreated groups. For this purpose, the cells were cultured on substrates with different elastic modulus. 24 hours after culture for untreated cells and 24 hours after treatment for treated cells, electron microscope photography was done. Fig. 5 shows the pictures taken of these cells.

In order to quantify the results, in several stages, cell images were given as input to Python code and Image J software, and the elongation index of cells was calculated. The image processing in Python code and Image J software was done in several steps. The amount of cell elongation index (circularity number) was calculated with Equation 1.

$$SI = \frac{4\pi A}{P^2} \tag{1}$$

Where A is the area, and P is the perimeter of each cell. This dimensionless index varies between 0 and 1. 0 is for completely elongated cells, and 1 is for entirely round cells.

Based on the Python code, the number of cells with different morphologies was measured, and the cells were counted in terms of number. Based on the circularity number, the cells were divided into four groups: 1. semi-elongated, 2. elongated, 3. round, and 4. semi-round. This code is based on color contrast, which gives better color contrast detection by trial-and-error adjustment of its variables.

Fig5A for the DU145 Cell line, the control sample had more elongated and semi-elongated cells. These cells, after the effect of different kinds of substrate, had a tendency to become semi-round and round morphology. The frequency of round cells was 32.92 ± 2.53, 27.84 ± 3.40, and 19.82 ± 1.59 in the soft sub, medium sub, and stiff sub, Respectively, which have increased significantly compared to the control (P:0.01, P:0.037 and P:0.0007 Respectively). Also, the frequency of semi-round cells was in the soft sub, medium sub, and stiff sub, respectively 39.76 ± 3.76, 34.05 ± 3.29, 26.14 ± 5.13, which have increased significantly compared to the control (P:0.0006, P:0.0004 and P:0.0251 Respectively). The number of these cells in the soft sub is more than the other two substrates, which shows that the soft sub increases the morphology of round and semi-round cells, and as a result, this soft sub kills more cancer cells. The number of elongated cells in the stiff sub was more than in the soft sub, P:0.04 (Fig5A).

Fig5 B for the LNCaP Cell line, the control sample had more elongated cells than other groups. These cells, after the effect of different kinds of substrate, had a tendency to become round morphology. The frequency of round cells was 30.84 ± 2.77, 21.51 ± 2.11, and 15.85 ± 2.05 in the soft sub, medium sub, and stiff sub, Respectively, which have increased significantly compared to the control (P:0.03, P:0.03, and P:0.005 Respectively). The stiff sub had a more significant number of cells elongating, as opposed to the soft sub and medium sub, where cells mainly were round (p:0.02) (Fig5 B). Our findings showed that cells on both stiff and soft sub tend to round at different rates during seeding time. The rate of rounding was higher for cells on soft sub.

Fig. 5A (DU145) shows the Frequency of different types of cells in the group under the substrate and also under the substrate with cells treated by drug. In all groups, a drug with substrate increased the number of round cells and decreased the number of elongated cells compared to the substrate with cells untreated, and this effect is not significant in all groups. The Frequency of round cells in the soft sub was 32.927 ± 2.531, and in the soft sub with drug number of these cells was increased (48.633 ± 0.302). This increase was statistically significant, with a p-value of 0.03. Also, the Frequency of round cells was higher in the medium sub with cells treated by drug (27.843 ±3.404) than in the medium sub with cells untreated (39.783 ± 3.285). This increase was statistically significant with a P<0.0001. On the other hand, the Frequency of elongated cells in the soft sub was 21.703 ± 1.470, and in the soft sub with cells treated by drug number of these cells decreased (8.190 ± 1.076). This decrease was statistically significant, with a p-value of 0.04. Part B (LNCaP), Significant changes were not observed in the drug groups with substrate compared to substrate with cells untreated in all cell morphology.

Fig. 6 shows the number of cells in morphological groups and different conditions. Figs. 6A and 6B show the effect of substrates on the morphology of DU145 and LNCAP cell lines, respectively. It can be seen that the percentage of the number of round cells on soft substrates is higher than the percentage of the number of round cells on medium and stiff substrates. Also, the percentage of elongated cells for both tested cell lines is higher for control group cells, cells cultured on stiff substrate, cells cultured on medium substrate, and cells cultured on soft substrate, respectively. Figs. 6C and 6D show the simultaneous effects of drugs and substrates on the morphology of DU145 and LNCAP cell lines, respectively. The effects of substrates in these two figures have the same trend for both treated and untreated cells and have the same trend as mentioned in the previous paragraph. Also, drugs increase the number of round cells and decrease the number of elongated cells in both cell lines and on all soft, medium, and stiff substrates.

*3.3 The results of examining live/dead cells by AO/PI staining*

In the previous section, the morphology of the cells was examined on different substrates in treated and untreated conditions. In order to find out what percentage of the cells are alive and what percentage are dead under the same conditions of morphology examination, in this section, the death rate of two cell lines, untreated and treated with Abiraterone Acetate drug and cultured on soft, medium and stiff substrates, has been investigated. In this study, acridine orange (AO) and propidium iodide (PI) staining were used to investigate the effect of different types of substrates and treatment of cells with drugs on cell death. AO is permeable to both living and dead cells and stains

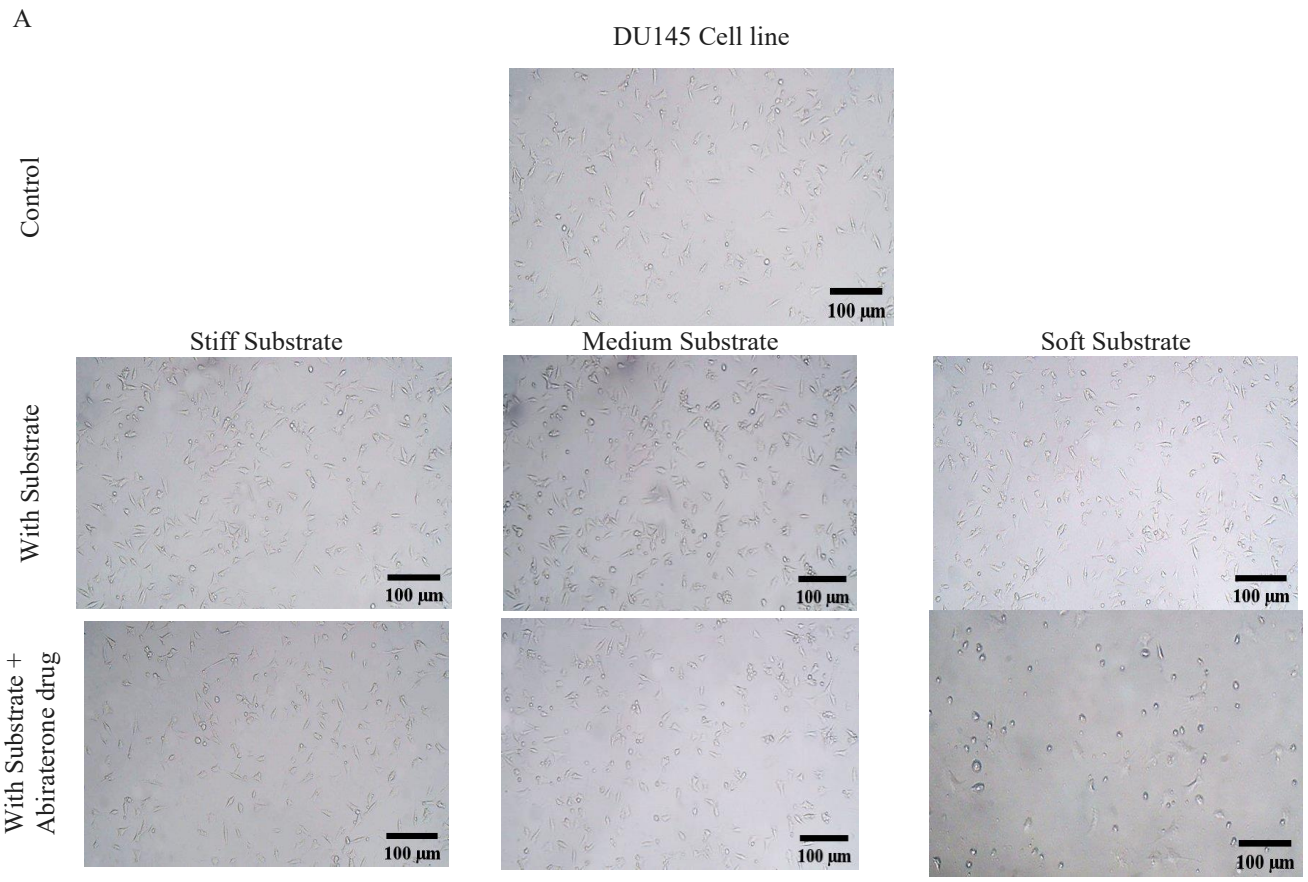


all nucleated cells with green fluorescent light. PI enters the dead cells through the damaged membrane and stains all dead nucleated cells to produce red fluorescence. In Fig. 7, the images obtained from the fluorescent microscope were given to investigate the effect of substrates and treated and untreated of two cell lines. In both cell lines, the number of dead cells in different substrates was higher than in the control sample, but with the addition of drugs to the substrate, the number of dead cells increased significantly.

Fig. 8 shows that in the DU145 cell line, the number of dead cells in the soft sub-group with cells treated by drug (45.24 ± 4.26) increased significantly compared to the control group (5.01) and the soft subgroup with cells untreated (7.74 ± 1.58) (P:0.01, P:0.02 respectively (Also, the number of dead cells in the medium sub-group with cells treated by drug (41.18 ± 2.59) increased significantly compared to the control group (5.01) and the medium sub-group with cells untreated (4.37 ± 2.12) (P:0.007, P:0.003 respectively). The number of dead cells in the stiff sub-group with cells treated by drug (19.31 ± 1.00) increased significantly compared to the control group (5.01) and the stiff sub-group untreated (5.03 ± 1.80) (P:0.007, P:0.008 respectively). Although the number of dead cells in different types of substrates with cells treated by drug was more than in the substrate with cells untreated, the number of dead cells in the soft substrate with cells treated by drug was more than in other substrates with cells treated by drug.

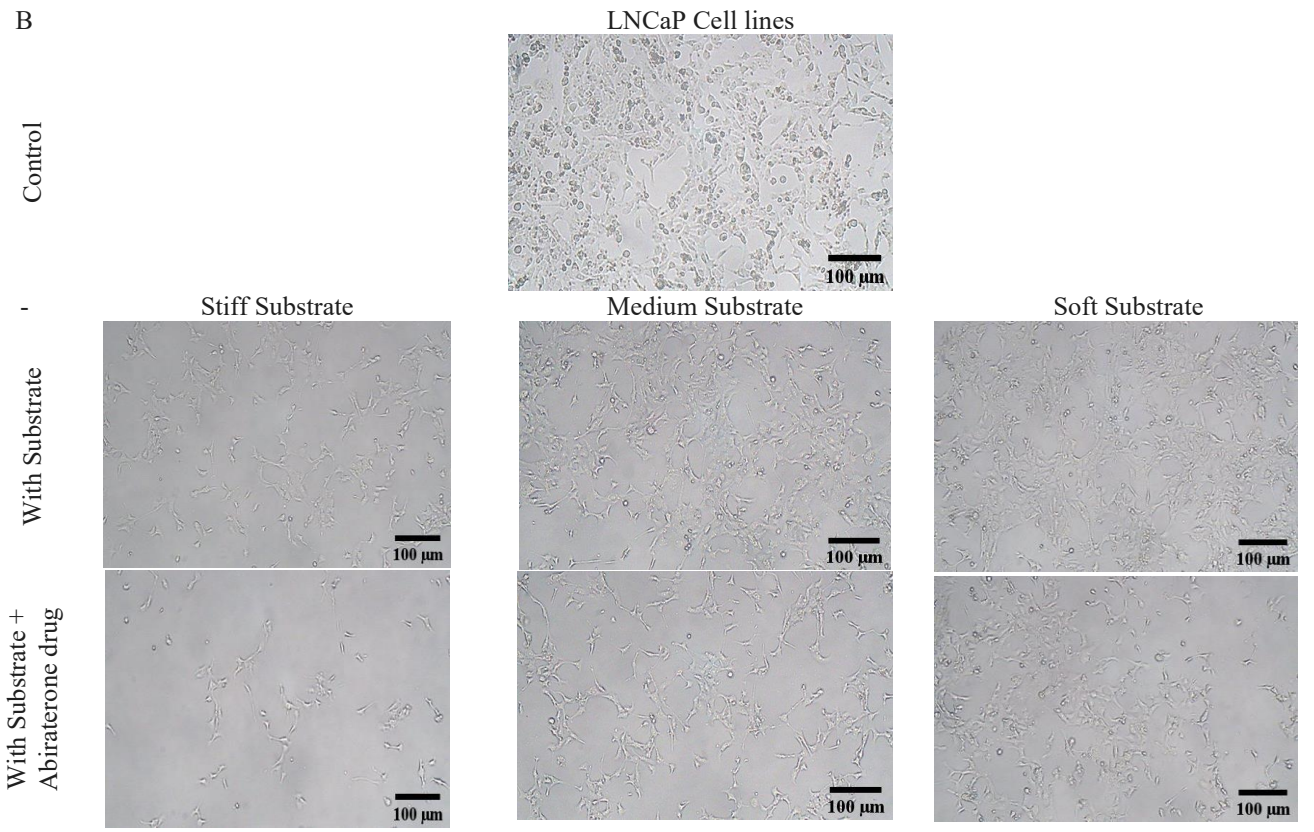


**Fig.5: The images of (A) DU 145 and (B) LNCAP cell lines for control groups, groups of cells treated and cultured on substrates, and groups of cells treated and cultured on substrates taken with an electron microscope.**

In the LNCaP cell line, the number of dead cells in the medium sub-group with cells treated by drug (33.87 ± 4.92) increased significantly compared to the control group (2.03) and the medium sub-group with cells untreated (5.91 ± 0.59) (P:0.03, P:0.04 respectively). Also, the number of dead cells in the stiff sub-group with cells treated by drug (19.31 ± 1.00) increased significantly compared to the control group (2.03) (P:0.04). As can be understood from Fig. 8, the percentage of dead cells in cells cultured on soft substrates is higher than in cells cultured on stiff substrates, and this difference is greater in treated cells than untreated cells. Also, the treatment of the cells has caused the death of most of the cells.

## 4. Discussion

The detection and identification of cancer cells based on their shape is extremely useful in the future therapy of these cells. Cells with varying degrees of invasion can metastasis and be found in different tissue of the body with varying elastic modulus, influencing cell morphology. Additionally, the impact of medications on cell morphology can aid in cell diagnostics and therapeutic efficacy. Since the groundbreaking studies using hydrogel or elastomer substrates of different stiffness that revealed changes in fibroblast morphology and motility in response to substrate elastic modulus, systematic research into cellular responses to the mechanical properties of their environment has progressed dramatically [29, 30], this work examined the effects of different substrate compositions on the circular morphology of two different cancer cell lines, both with and without Abiraterone acetate drug. A computer study based on Python was used to quantify the quantity of cells with various morphologies. Based on circularity metrics, cells were then divided into four groups: 1. semi-elongated, 2. elongated, 3. round, and 4. semi-round.

The IC50 calculation used to evaluate cell viability revealed significant differences between the way the medication affected the DU145 and LNCaP cell lines. Notably, the medication appears to have a more cytotoxic effect on DU145 cells than LNCaP cells, as indicated by the computed IC50 values of 110.9µM for DU145 and 328.3µM for LNCaP.

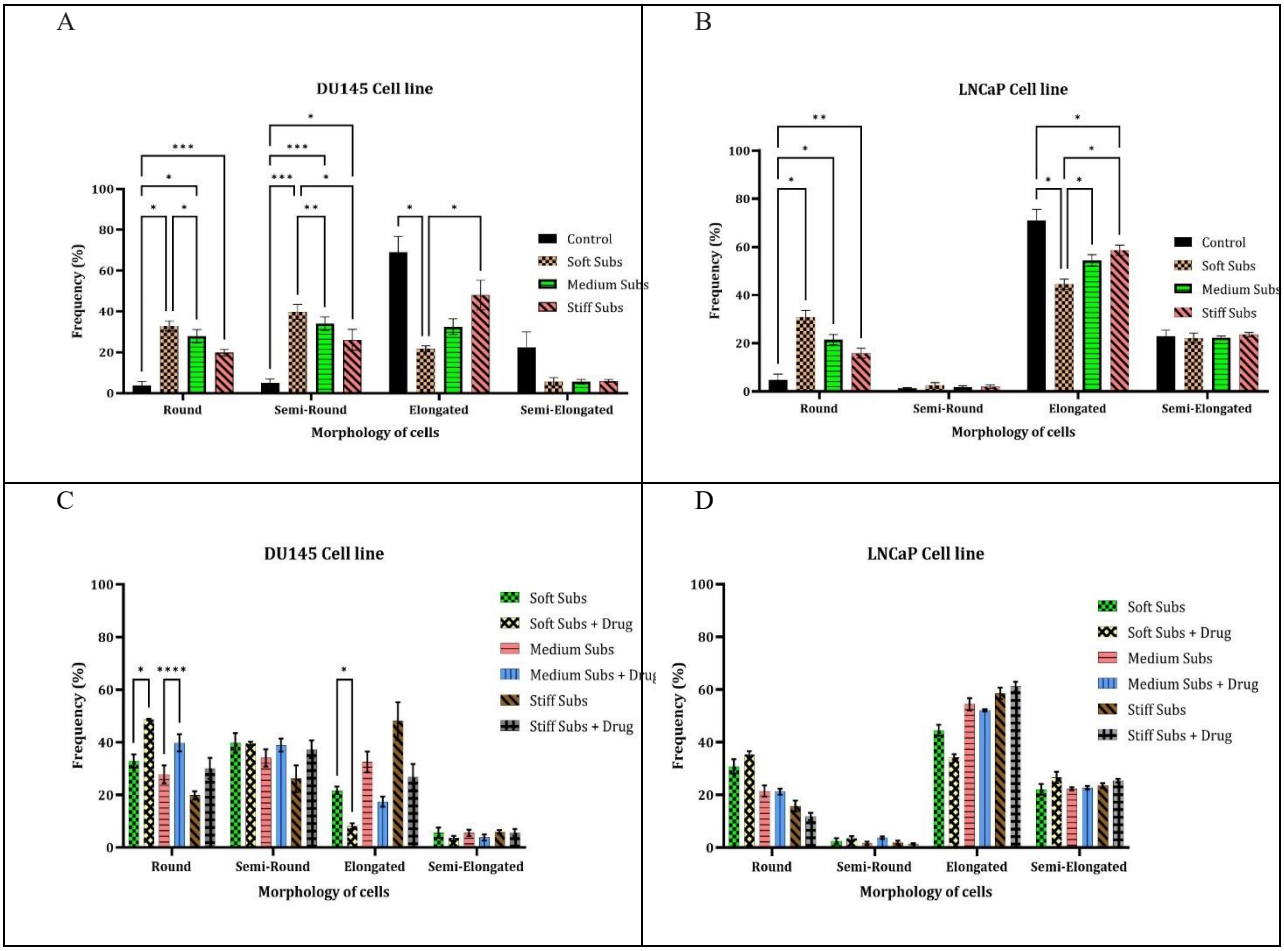


**Fig6: Number of cells in morphological groups and different conditions. Effect of substrates on the morphology for (A) DU145 and (B) LNCAP cell lines. Also, simultaneous effects of drugs and substrates on the morphology for (C) DU145 and (D) LNCAP cell lines. Significant differences between groups were determined by Tukey's test, and the * indicates the p-value between groups. (* P<0.05, ** P<0.01, *** P<0.001)**

The impact of substrate stiffness on cell morphology has been well documented for a wide range of materials, including silicone films, rubber-like elastomers like polydimethylsiloxane (PDMS) or polyurethanes, needle-shaped pillar arrays made of PDMS, silicon, or glass, and hydrogels made of DNA, agarose, hyaluronic acid, polyethylene glycol (PEG), crosslinked polyacrylamide, and other flexible water-soluble polymers [31-41]. The way that different cell types react to stiffness in the matrix varies greatly and depends on the type of adhesion receptor the cell uses to communicate with its substrate. Significant differences are also found between cells grown on two- and three-dimensional sticky materials. However, the substrate's elastic modulus has a significant impact on cell shape and protein expression across a broad range, even when it is limited to adhesion on planar surfaces [42].

Understanding the morphological changes brought about by various substrates—both with and without Abiraterone acetate drug—provided important information on how cells reacted. DU145 cells showed a significant change toward round and semi-round morphologies after being exposed to substrates; this movement was most pronounced on the soft substrate. On the other hand, LNCaP cells primarily exhibited a spherical shape on all surfaces, with a greater tendency to round on the pliable substrate. DU145 cells exhibited a notable promotion of cell elongation due to the stiff substrate, indicating that the effects of substrate stiffness on cell shape vary throughout cell lines.

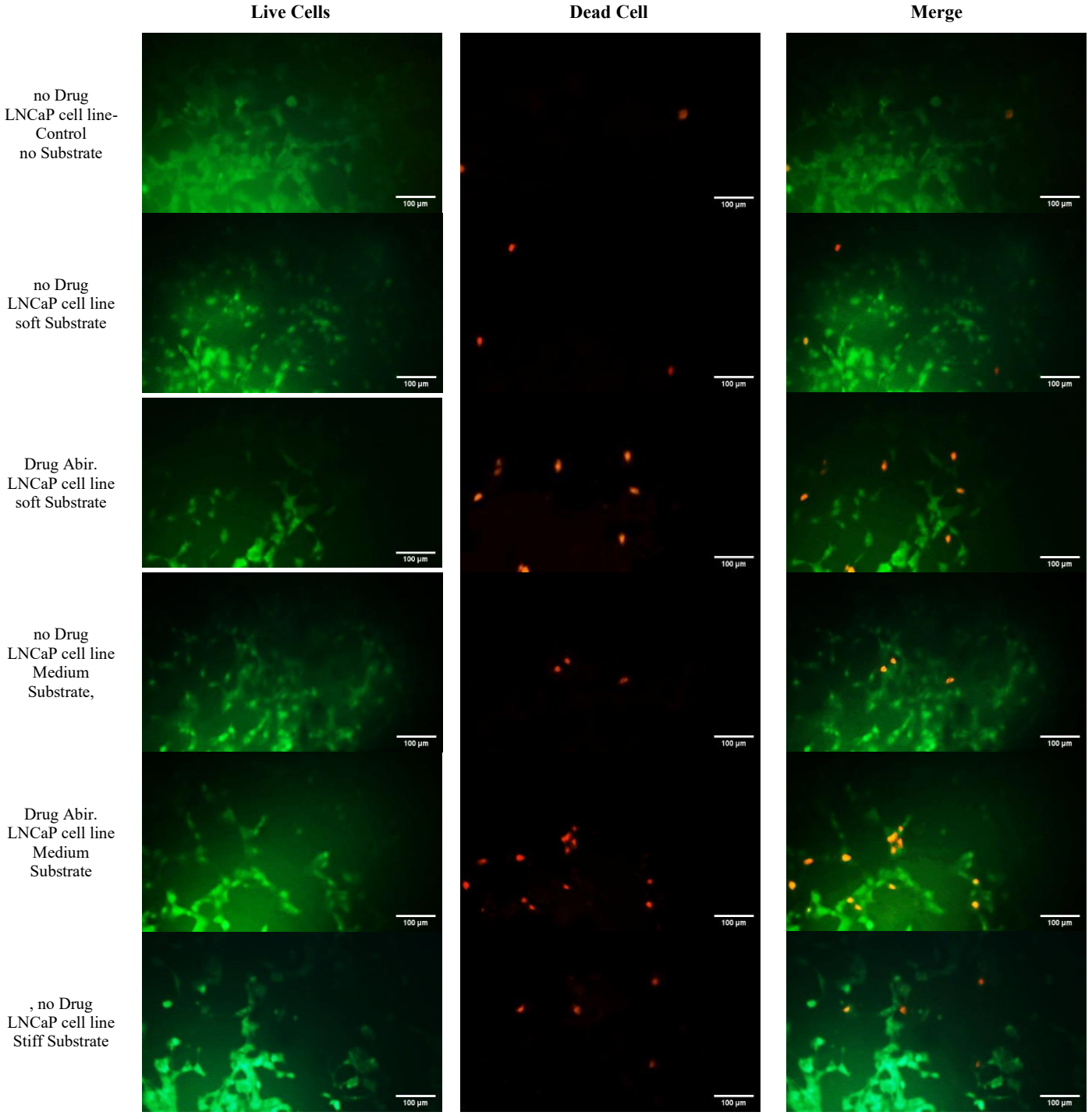
Live Cells
Dead Cell
Merge
no Drug LNCaP cell line- Control no Substrate
no Drug LNCaP cell line soft Substrate
Drug Abir. LNCaP cell line soft Substrate
no Drug LNCaP cell line Medium Substrate,
Drug Abir. LNCaP cell line Medium Substrate
, no Drug LNCaP cell line Stiff Substrate
100 µm

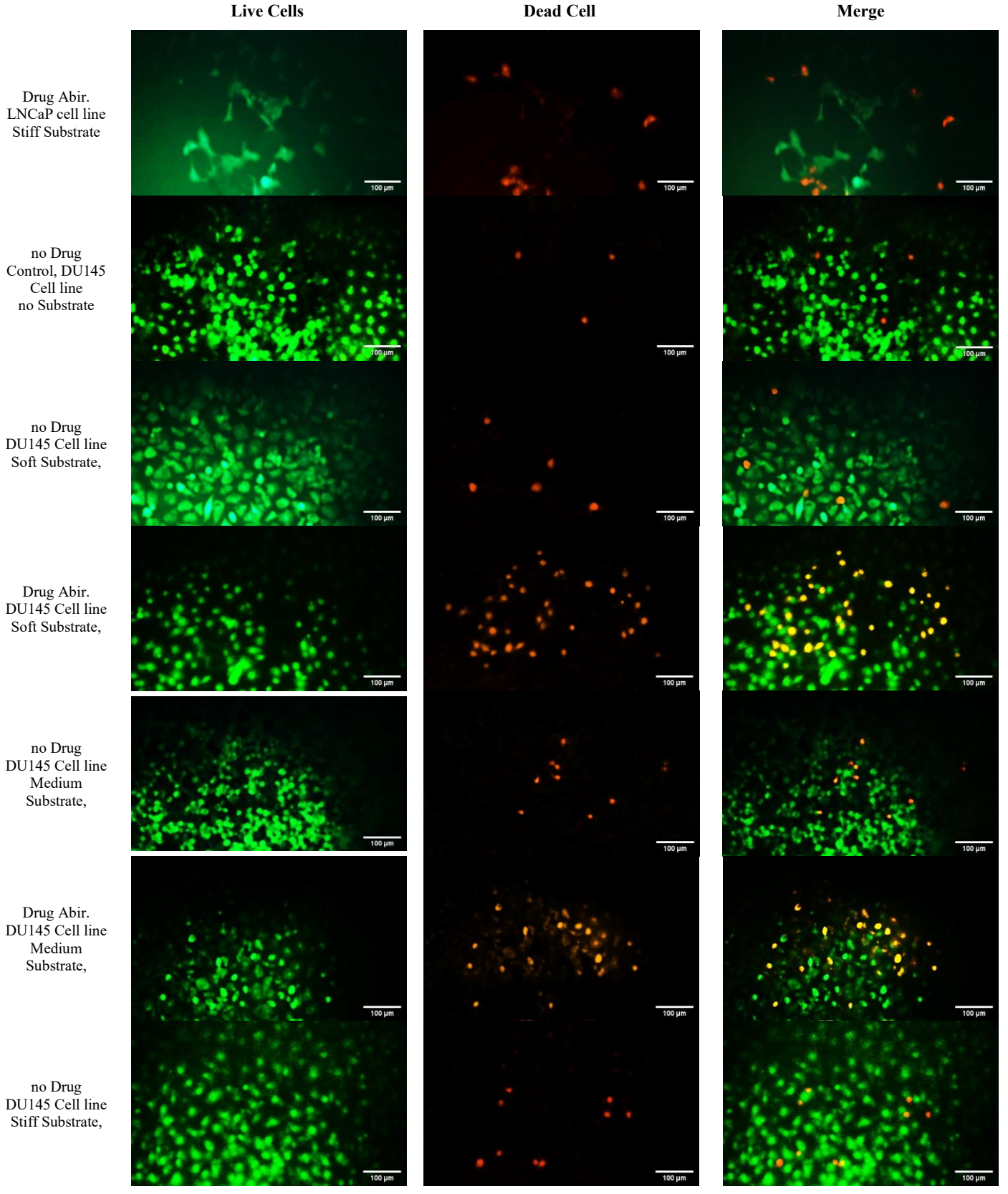
Live Cells
Dead Cell
Merge
Drug Abir. LNCaP cell line Stiff Substrate
no Drug Control, DU145 Cell line no Substrate
no Drug DU145 Cell line Soft Substrate,
Drug Abir. DU145 Cell line Soft Substrate,
no Drug DU145 Cell line Medium Substrate,
Drug Abir. DU145 Cell line Medium Substrate,
no Drug DU145 Cell line Stiff Substrate,
100 µm

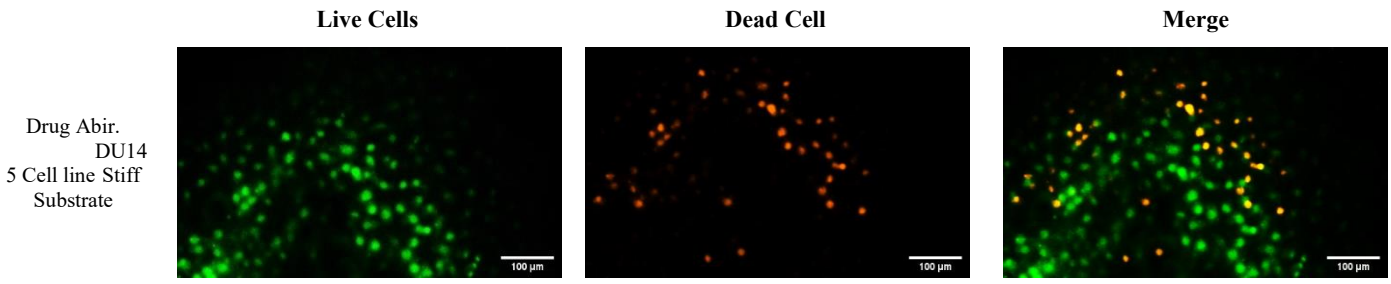


**Fig 7: Prostate cancer cells (DU145 and LNCaP) with varying levels of invasion were imaged using live/dead techniques. The cells were grown on substrates of variable stiffness (soft, medium, and stiff) and were either untreated or treated with Abiraterone Acetate medicines. Live cells are represented by the colour green, whereas dead cells are represented by the colour red.**

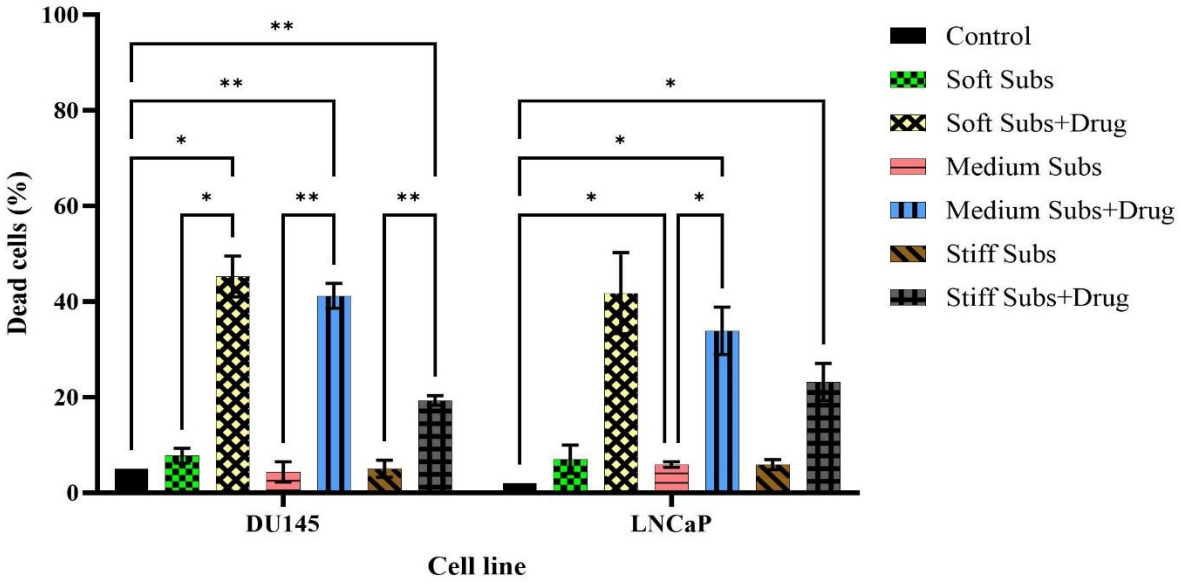


**Fig 8: The percentage of deceased cells assessed in the live/dead assay was measured in the control group and on cultured on substrates with varied levels of stiffness, namely (a) soft, (b) medium, and (c) stiff, both before and after medication for two cell lines DU145 and LNCaP. Statistical differences between the control group and the various experimental groups were determined by Tukey's test, and the * indicates the p-value between groups. (* P<0.05, ** P<0.01)**

In the soft, medium, and stiff substrates for the DU145 cell line, the frequencies of round cells were 32.92 ± 2.53, 27.84 ± 3.40, and 19.82 ± 1.59, respectively. These values showed significant increases over the control (P: 0.01, P: 0.037, and P: 0.0007, respectively). Furthermore, there were notable increases in the frequencies of semi-round cells compared to the control (P: 0.0006, P: 0.0004, and P: 0.0251) in the soft, medium, and stiff substrates, which were 39.76 ± 3.76, 34.05 ± 3.29, and 26.14 ± 5.13, respectively. Round cell frequencies for the LNCaP cell line were 30.84 ± 2.77, 21.51 ± 2.11, and 15.85 ± 2.05 in the soft, medium, and stiff substrates, respectively. These values were considerably higher than those of the control (P: 0.03, P: 0.03, and P: 0.005, respectively). Moreover, the stiff substrate induced a more significant number of elongated cells compared to the soft and medium substrates, where cells were predominantly round (P: 0.02).

Pathological circumstances are essential drivers of disease progression because they frequently lead to aberrant and extensive ECM deposition and remodeling [43, 44]. The ECM is inherently changed in tumors, and this greatly

accelerates the course of the disease. Compared to normal tissue, ECM modification is notable since it was one of the first indicators of carcinogenesis. These changes are now known to be distinctive characteristics of solid tumors [45-47]. Host stromal cells, such as tumor-associated macrophages or cancer-associated fibroblasts, are recruited by cancer cells and contribute in different ways to the remodeling of ECM. These stromal cells degrade and reorganize the preexisting ECM in addition to synthesizing new components and releasing remodeling enzymes [48-51]. Consequently, these processes lead to the formation of a pervasive, dense fibrous tissue that typically envelops the tumor and contributes to the observed increase in local tissue stiffness within the tumor microenvironment. Indeed, this remodeling activity persists continuously, resulting in progressive stiffening of the ECM within the tumor milieu over time [52, 53].

Although not consistently significant across all scenarios, the introduction of the medication, together with substrates, led to a decrease in the number of elongated cells and an increase in round cells. On the other hand, co-administration of the medication resulted in a significant rise in round cells and a decrease in elongated cells for DU145 cells cultivated on the soft substrate, suggesting increased cell death.

Acridine orange (AO) and propidium iodide (PI) staining analysis of cell death offered additional proof of the drug's cytotoxic effects. The medication with substrates caused a notable rise in the percentage of dead cells in both cell lines. Particularly noteworthy was the pronounced increase in cell death observed in DU145 cells on the soft substrate when treated with the drug compared to other substrate-drug combinations.

In the DU145 cell line, the soft substrate group treated with the medication had a substantially higher number of dead cells (45.24 ± 4.26) than both the control group (5.01) and the soft substrate group by itself (7.74 ± 1.58) (P: 0.01, P: 0.02, respectively). Comparably, the number of dead cells (41.18 ± 2.59) in the drug-treated medium substrate group greatly outnumbered that of the control group (5.01) and the medium substrate group by itself (4.37 ± 2.12) (P: 0.007, P: 0.003, respectively). Furthermore, the number of dead cells (19.31 ± 1.00) in the drug-treated stiff substrate group was substantially higher than that of the control group (5.01) and the stiff substrate group by itself (5.03 ± 1.80) (P: 0.007, P: 0.008, respectively). While the number of dead cells was generally higher in the substrate-drug combinations compared to substrate with cells untreated, the soft substrate with cells treated by drug exhibited the highest number of dead cells among all substrate-drug combinations.

The number of dead cells in the drug-treated medium substrate group (33.87 ± 4.92) in the LNCaP cell line was considerably higher than that of the control group (2.03) and the medium substrate group by itself (5.91 ± 0.59) (P: 0.03, P: 0.04, respectively). Comparably, the number of dead cells (19.31 ± 1.00) in the stiff substrate group treated with the medication was considerably higher than that of the control group (2.03; P = 0.04).

These findings highlight the critical influence that medication interactions and substrate characteristics have on determining cell survival and morphology. The observed differences in responses between the LNCaP and DU145 cell lines highlight the need for customized therapeutic approaches in the treatment of cancer, taking into account the various features of cancer cell populations and their microenvironmental settings.

Research employing human prostate cancer cell lines LNCaP and DU145 has revealed that prostate cancer cell motility is increased with the establishment of a versican-rich pericellular matrix, which may facilitate the development of locally invasive illness [54]. Furthermore, it has been noted that the stromal milieu of human prostate cancer exhibits elevated expression of the glycoprotein tenascin-C [55, 56]. Growing evidence underscores the pivotal role of ECM stiffening as a critical determinant of tumor growth, invasion, and metastasis, particularly in prostate cancer [57, 58]. From early stages to metastatic disease, growing evidence highlights an apparent relationship between prostate tumors, ECM component changes, and tissue stiffness. At a cellular level, stiff matrices are shown to induce a phenotypic switch in metastatic cancer cells, which is accompanied by an increase in drug resistance. These highlight the role of mechanical cues not only in disease progression but also in response to treatment [59]. Research on the temporal dynamics of mechanosensing is still underway. Previous research using epithelial cells grown on polyacrylamide gels with different elastic moduli has seen this effect. The body of research on the effect of substrate stiffness on cellular behavior generally points to the importance of substrate stiffness in determining cell activity [60-63]. Many studies have also paid attention to the effect of substrate properties on the behavior of cells and their mechanical properties and show that substrate stiffness can affect cell properties and their behavior [64-66].

Also the interaction between substrate stiffness and Abiraterone Acetate may affect the morphology and viability of prostate cancer cells through mechanical and cell adhesion pathways, the YAP/TAZ mechanotransduction pathway, apoptosis, or the PI3K/AKT/mTOR pathway.

Cancer cells utilize integrins and focal adhesion kinase (FAK) to interact with the extracellular matrix (ECM), which is critical for their survival and metastatic potential. On stiff substrates, integrin expression and FAK activation are increased, enhancing cell adhesion and cytoskeletal stability, whereas soft substrates result in decreased integrin signaling, increased cell rounding, and increased apoptosis susceptibility. Stiff ECM enhances integrin-mediated signaling, leading to increased cell survival and metastatic behavior [67, 68]. Mechanotransduction

pathways, including β1-integrin and FAK, are critical for maintaining stem-like properties in prostate cancer [67]. Abiraterone acetate, an androgen receptor inhibitor, may alter integrin expression and affect cell adhesion and survival mechanisms [69]. Drug efficacy can be influenced by the mechanical properties of the substrate, potentially affecting treatment outcomes [70, 71].

On stiff substrates, YAP/TAZ is activated, increasing cell survival and resistance to drug treatments. Conversely, soft substrates reduce YAP/TAZ activity and increase cell sensitivity to environmental stresses, including drug-induced apoptosis. Stiff substrates increase YAP/TAZ nuclear translocation, leading to increased expression of genes associated with cell survival and proliferation [67, 72, 73]. Reduced mechanical signaling on soft substrates may facilitate apoptosis, making these environments potentially more effective for therapeutic interventions [74]. Research suggests that softer substrates may enhance apoptotic signaling. On softer substrates, increased expression of the pro-apoptotic proteins BAX and BAK leads to mitochondrial permeability, cytochrome c release, and caspases activation, leading to cell death. Soft environments may increase the expression of death receptors such as Fas and TRAIL-R and increase susceptibility to apoptosis through caspase-8 activation [75-77].

Stiff substrates can activate pathways that promote cell survival and drug resistance, particularly the PI3K/AKT/mTOR pathway, which may reduce the efficacy of Abiraterone Acetate by promoting cell proliferation and reducing apoptosis. This response may be further mediated by hypoxia-related pathways, such as HIF-1α, which also contribute to drug resistance in mechanically harsh environments. Stiff substrates have been associated with increased activation of the PI3K/AKT/mTOR pathway, which is critical for cell survival and proliferation in prostate cancer [78, 79]. Dysregulation of this pathway is common in advanced prostate cancer and leads to resistance to therapies such as Abiraterone Acetate [80]. HIF-1α expression is increased in harsh environments, enhancing cell survival and reducing drug-induced apoptosis. The TGF-β pathway also plays a role in increasing drug resistance and cell invasion under these conditions [78, 81, 82]

## 5. Conclusions

Significant results were obtained from the study examining the effects of substrate stiffness and chemical drug abiraterone acetate on cell viability and morphology in DU145 and LNCaP cell lines. The IC50 results showed that the medication was more hazardous to DU145 cells than to LNCaP cells, which may indicate that various prostate cancer cell lines had varying drug sensitivity. The examination of cell morphology demonstrated unique reactions to both drug treatment and substrate stiffness. Substrates caused a shift in the morphology of DU145 cells toward round and semi-round shapes; this shift was especially noticeable on the soft substrate. On the other hand, LNCaP cells exhibited a tendency towards a spherical shape on all surfaces, with a discernible difference in elongation on rigid substrates. In both cell lines, combining the medication with substrates led to a decrease in elongated cells and an increase in round cells. However, the statistical significance differed. Significantly, the drug-treated soft substrate showed a drop in elongated cells and an increase in round cells, suggesting a strong cytotoxic effect. Evaluation of cell death highlighted the medication and substrates' synergistic effects even more. The drug's soft substrate caused the most significant rise in dead cells in the DU145 and LNCaP cell lines, demonstrating how effective it is at inducing cell death.

Our research concludes by highlighting the significance of medication interactions and substrate properties in modifying prostate cancer cell behavior. Comprehending these dynamics is essential for formulating focused, therapeutic approaches customized to the distinct attributes of cancerous cells, hence potentially enhancing treatment results in patients with prostate cancer with differing metastatic propensities. To completely understand the therapeutic potential of substrate stiffness modulation in combination with anti-cancer medications, more investigation into the underlying mechanisms causing these effects is necessary.

## References

[1] S. Iyer, R. Gaikwad, V. Subba-Rao, C. Woodworth, I. Sokolov, Atomic force microscopy detects differences in the surface brush of normal and cancerous cells, *Nature nanotechnology,* Vol. 4, No. 6, pp. 389-393, 2009.

[2] C.-H. Hsieh, Y.-H. Lin, S. Lin, J.-J. Tsai-Wu, C. H. Wu, C.-C. Jiang, Surface ultrastructure and mechanical property of human chondrocyte revealed by atomic force microscopy, *Osteoarthritis and cartilage,* Vol. 16, No. 4, pp. 480-488, 2008.

[3] K. Dastani, M. Moghimi Zand, A. Hadi, Dielectrophoretic effect of nonuniform electric fields on the protoplast cell, *Journal of Computational Applied Mechanics,* Vol. 48, No. 1, pp. 1-14, 2017.

[4] D. Vignjevic, G. Montagnac, Reorganisation of the dendritic actin network during cancer cell migration and invasion, in *Proceeding of,* Elsevier*,* pp. 12-22.

[5] A. Kordzadeh, S. Javdansirat, N. Javdansirat, H. Tang, S. Ghaderi, A. Hadi, R. Mahmoudi, M. Nikseresht, Investigating Heat-Induced Phase Transitions in POPC Lipid Bilayers Using Molecular Dynamics Simulations, *Journal of Computational Applied Mechanics,* Vol. 55, No. 4, pp. 771-782, 2024.

[6] N. Miyoshi, H. Tanabe, T. Suzuki, K. Saeki, Y. Hara, Applications of a standardized green tea catechin preparation for viral warts and human papilloma virus-related and unrelated cancers, *Molecules,* Vol. 25, No. 11, pp. 2588, 2020.

[7] S. K. Tyring, Effect of Sinecatechins on HPV-Activated Cell Growth and Induction of Apoptosis, *J Clin Aesthet Dermatol,* Vol. 5, No. 2, pp. 34-41, Feb, 2012. eng

[8] Y. Hara, Tea catechins and their applications as supplements and pharmaceutics, *Pharmacol Res,* Vol. 64, No. 2, pp. 100-4, Aug, 2011. eng

[9] M. S. Chapekar, Tissue engineering: challenges and opportunities, *Journal of Biomedical Materials Research: An Official Journal of The Society for Biomaterials, The Japanese Society for Biomaterials, and The Australian Society for Biomaterials and the Korean Society for Biomaterials,* Vol. 53, No. 6, pp. 617-620, 2000.

[10] T.-H. Chang, H.-D. Huang, W.-K. Ong, Y.-J. Fu, O. K. Lee, S. Chien, J. H. Ho, The effects of actin cytoskeleton perturbation on keratin intermediate filament formation in mesenchymal stem/stromal cells, *Biomaterials,* Vol. 35, No. 13, pp. 3934-3944, 2014.

[11] D. Lü, C. Luo, C. Zhang, Z. Li, M. Long, Differential regulation of morphology and stemness of mouse embryonic stem cells by substrate stiffness and topography, *Biomaterials,* Vol. 35, No. 13, pp. 3945-3955, 2014/04/01/, 2014.

[12] L. Trichet, J. Le Digabel, R. J. Hawkins, S. R. K. Vedula, M. Gupta, C. Ribrault, P. Hersen, R. Voituriez, B. Ladoux, Evidence of a large-scale mechanosensing mechanism for cellular adaptation to substrate stiffness, *Proceedings of the National Academy of Sciences,* Vol. 109, No. 18, pp. 6933-6938, 2012.

[13] N. Mahmoodi, J. Ai, Z. Hassannejad, S. Ebrahimi-Barough, E. Hasanzadeh, A. Hadi, H. Nekounam, V. Rahimi-Movaghar, Are reported methods for synthesizing nanoparticles and microparticles by magnetic stirrer reproducible?, *Journal of Computational Applied Mechanics,* Vol. 51, No. 2, pp. 498-500, 2020.

[14] A. Korolj, C. Laschinger, C. James, E. Hu, C. Velikonja, N. Smith, I. Gu, S. Ahadian, R. Willette, M. Radisic, Curvature facilitates podocyte culture in a biomimetic platform, *Lab on a Chip,* Vol. 18, No. 20, pp. 3112-3128, 2018.

[15] P. A. Janmey, R. T. Miller, Mechanisms of mechanical signaling in development and disease, *Journal of cell science,* Vol. 124, No. 1, pp. 9-18, 2011.

[16] S. R. Caliari, J. A. Burdick, A practical guide to hydrogels for cell culture, *Nature methods,* Vol. 13, No. 5, pp. 405-414, 2016.

[17] K. Lee, F. Forudi, G. M. Saidel, M. S. Penn, Alterations in internal elastic lamina permeability as a function of age and anatomical site precede lesion development in apolipoprotein E–null mice, *Circulation research,* Vol. 97, No. 5, pp. 450-456, 2005.

[18] M. CM, Normal vascular aging: Differential effects on wave reflection and aortic pulse wave velocity, *J Am Coll Cardiol,* Vol. 46, pp. 1753-1760, 2005.

[19] S. R. Ramezani, A. Mojra, M. Tafazzoli-Shadpour, Investigating the effects of substrate stiffness on half-maximal inhibitory concentration of chemical anticancer drugs, cell viability and migration of cell lines, *Cellular, Molecular and Biomedical Reports*, pp. 141-147, 2024.

[20] S. Au - Syed, A. Au - Karadaghy, S. Au - Zustiak, Simple Polyacrylamide-based Multiwell Stiffness Assay for the Study of Stiffness-dependent Cell Responses, *JoVE*, No. 97, pp. e52643, 2015/03/25/, 2015.

[21] R. G. Wells, The role of matrix stiffness in regulating cell behavior, *Hepatology,* Vol. 47, No. 4, pp. 1394-1400, 2008.

[22] Q. Chai, Y. Jiao, X. Yu, Hydrogels for biomedical applications: their characteristics and the mechanisms behind them, *Gels,* Vol. 3, No. 1, pp. 6, 2017.

[23] E. Caló, V. V. Khutoryanskiy, Biomedical applications of hydrogels: A review of patents and commercial products, *European polymer journal,* Vol. 65, pp. 252-267, 2015.

[24] M. Bassil, J. Davenas, M. E. Tahchi, Electrochemical properties and actuation mechanisms of polyacrylamide hydrogel for artificial muscle application, *Sensors and Actuators B: Chemical,* Vol. 134, No. 2, pp. 496-501, 2008.

[25] M. Bassil, M. Ibrahim, M. El Tahchi, Artificial muscular microfibers: hydrogel with high speed tunable electroactivity, *Soft Matter,* Vol. 7, No. 10, pp. 4833-4838, 2011.

[26] N. Chirani, L. Yahia, L. Gritsch, F. L. Motta, S. Chirani, S. Farè, History and applications of hydrogels, *Journal of biomedical sciences,* Vol. 4, No. 02, pp. 1-23, 2015.

[27] K. S. Kim, C. H. Cho, E. K. Park, M.-H. Jung, K.-S. Yoon, H.-K. Park, AFM-detected apoptotic changes in morphology and biophysical property caused by paclitaxel in Ishikawa and HeLa cells, *PloS one,* Vol. 7, No. 1, pp. e30066, 2012.

[28] C.-C. K. Lin, C.-H. Yang, M.-S. Ju, Cytotoxic and biomechanical effects of clinical dosing schemes of paclitaxel on neurons and cancer cells, *Cancer Chemotherapy and Pharmacology,* Vol. 86, pp. 245-255, 2020.

[29] A. K. Harris, D. Stopak, P. Wild, Fibroblast traction as a mechanism for collagen morphogenesis, *Nature,* Vol. 290, No. 5803, pp. 249-51, Mar 19, 1981. eng

[30] A. K. Harris, P. Wild, D. Stopak, Silicone rubber substrata: a new wrinkle in the study of cell locomotion, *Science,* Vol. 208, No. 4440, pp. 177-9, Apr 11, 1980. eng

[31] C. X. Li, N. P. Talele, S. Boo, A. Koehler, E. Knee-Walden, J. L. Balestrini, P. Speight, A. Kapus, B. Hinz, MicroRNA-21 preserves the fibrotic mechanical memory of mesenchymal stem cells, *Nat Mater,* Vol. 16, No. 3, pp. 379-389, Mar, 2017. eng

[32] A. Zhong, Z. Mirzaei, C. A. Simmons, The Roles of Matrix Stiffness and ß-Catenin Signaling in Endothelial-to-Mesenchymal Transition of Aortic Valve Endothelial Cells, *Cardiovasc Eng Technol,* Vol. 9, No. 2, pp. 158-167, Jun, 2018. eng

[33] T. Tzvetkova-Chevolleau, A. Stéphanou, D. Fuard, J. Ohayon, P. Schiavone, P. Tracqui, The motility of normal and cancer cells in response to the combined influence of the substrate rigidity and anisotropic microstructure, *Biomaterials,* Vol. 29, No. 10, pp. 1541-51, Apr, 2008. eng

[34] Y. Andriani, J. M. Chua, B. Y. Chua, I. Y. Phang, N. Shyh-Chang, W. S. Tan, Polyurethane acrylates as effective substrates for sustained in vitro culture of human myotubes, *Acta Biomater,* Vol. 57, pp. 115-126, Jul 15, 2017. eng

[35] L. Cacopardo, N. Guazzelli, R. Nossa, G. Mattei, A. Ahluwalia, Engineering hydrogel viscoelasticity, *J Mech Behav Biomed Mater,* Vol. 89, pp. 162-167, Jan, 2019. eng

[36] E. Migliorini, J. Ban, G. Grenci, L. Andolfi, A. Pozzato, M. Tormen, V. Torre, M. Lazzarino, Nanomechanics controls neuronal precursors adhesion and differentiation, *Biotechnol Bioeng,* Vol. 110, No. 8, pp. 2301-10, Aug, 2013. eng

[37] C. E. Kandow, P. C. Georges, P. A. Janmey, K. A. Beningo, Polyacrylamide hydrogels for cell mechanics: steps toward optimization and alternative uses, *Methods Cell Biol,* Vol. 83, pp. 29-46, 2007. eng

[38] T. Okamoto, Y. Takagi, E. Kawamoto, E. J. Park, H. Usuda, K. Wada, M. Shimaoka, Reduced substrate stiffness promotes M2-like macrophage activation and enhances peroxisome proliferator-activated receptor γ expression, *Exp Cell Res,* Vol. 367, No. 2, pp. 264-273, Jun 15, 2018. eng

[39] P. Zarrintaj, S. Manouchehri, Z. Ahmadi, M. R. Saeb, A. M. Urbanska, D. L. Kaplan, M. Mozafari, Agarose-based biomaterials for tissue engineering, *Carbohydr Polym,* Vol. 187, pp. 66-84, May 1, 2018. eng

[40] A. Bauer, L. Gu, B. Kwee, W. A. Li, M. Dellacherie, A. D. Celiz, D. J. Mooney, Hydrogel substrate stress-relaxation regulates the spreading and proliferation of mouse myoblasts, *Acta Biomater,* Vol. 62, pp. 82-90, Oct 15, 2017. eng

[41] M. Bao, J. Xie, N. Katoele, X. Hu, B. Wang, A. Piruska, W. T. S. Huck, Cellular Volume and Matrix Stiffness Direct Stem Cell Behavior in a 3D Microniche, *ACS Appl Mater Interfaces,* Vol. 11, No. 2, pp. 1754-1759, Jan 16, 2019. eng

[42] T. Yeung, P. C. Georges, L. A. Flanagan, B. Marg, M. Ortiz, M. Funaki, N. Zahir, W. Ming, V. Weaver, P. A. Janmey, Effects of substrate stiffness on cell morphology, cytoskeletal structure, and adhesion, *Cell Motil Cytoskeleton,* Vol. 60, No. 1, pp. 24-34, Jan, 2005. eng

[43] F. Martino, A. R. Perestrelo, V. Vinarský, S. Pagliari, G. Forte, Cellular Mechanotransduction: From Tension to Function, *Front Physiol,* Vol. 9, pp. 824, 2018. eng

[44] L. Martinez-Vidal, V. Murdica, C. Venegoni, F. Pederzoli, M. Bandini, A. Necchi, A. Salonia, M. Alfano, Causal contributors to tissue stiffness and clinical relevance in urology, *Commun Biol,* Vol. 4, No. 1, pp. 1011, Aug 26, 2021. eng

[45] Y. F. I. Setargew, K. Wyllie, R. D. Grant, J. L. Chitty, T. R. Cox, Targeting Lysyl Oxidase Family Meditated Matrix Cross-Linking as an Anti-Stromal Therapy in Solid Tumours, *Cancers (Basel),* Vol. 13, No. 3, Jan 27, 2021. eng

[46] M. W. Pickup, J. K. Mouw, V. M. Weaver, The extracellular matrix modulates the hallmarks of cancer, *EMBO Rep,* Vol. 15, No. 12, pp. 1243-53, Dec, 2014. eng

[47] B. Emon, J. Bauer, Y. Jain, B. Jung, T. Saif, Biophysics of Tumor Microenvironment and Cancer Metastasis - A Mini Review, *Comput Struct Biotechnol J,* Vol. 16, pp. 279-287, 2018. eng

[48] J. Winkler, A. Abisoye-Ogunniyan, K. J. Metcalf, Z. Werb, Concepts of extracellular matrix remodelling in tumour progression and metastasis, *Nat Commun,* Vol. 11, No. 1, pp. 5120, Oct 9, 2020. eng

[49] V. Poltavets, M. Kochetkova, S. M. Pitson, M. S. Samuel, The Role of the Extracellular Matrix and Its Molecular and Cellular Regulators in Cancer Cell Plasticity, *Front Oncol,* Vol. 8, pp. 431, 2018. eng

[50] N. M. Anderson, M. C. Simon, The tumor microenvironment, *Curr Biol,* Vol. 30, No. 16, pp. R921-r925, Aug 17, 2020. eng

[51] T. R. Cox, The matrix in cancer, *Nat Rev Cancer,* Vol. 21, No. 4, pp. 217-238, Apr, 2021. eng

[52] A. M. Socovich, A. Naba, The cancer matrisome: From comprehensive characterization to biomarker discovery, *Semin Cell Dev Biol,* Vol. 89, pp. 157-166, May, 2019. eng

[53] K. R. Levental, H. Yu, L. Kass, J. N. Lakins, M. Egeblad, J. T. Erler, S. F. Fong, K. Csiszar, A. Giaccia, W. Weninger, M. Yamauchi, D. L. Gasser, V. M. Weaver, Matrix crosslinking forces tumor progression by enhancing integrin signaling, *Cell,* Vol. 139, No. 5, pp. 891-906, Nov 25, 2009. eng

[54] C. Ricciardelli, D. L. Russell, M. P. Ween, K. Mayne, S. Suwiwat, S. Byers, V. R. Marshall, W. D. Tilley, D. J. Horsfall, Formation of hyaluronan- and versican-rich pericellular matrix by prostate cancer cells promotes cell motility, *J Biol Chem,* Vol. 282, No. 14, pp. 10814-25, Apr 6, 2007. eng

[55] W. D. Ni, Z. T. Yang, C. A. Cui, Y. Cui, L. Y. Fang, Y. H. Xuan, Tenascin-C is a potential cancer-associated fibroblasts marker and predicts poor prognosis in prostate cancer, *Biochem Biophys Res Commun,* Vol. 486, No. 3, pp. 607-612, May 6, 2017. eng

[56] B. F. Gonçalves, S. G. Campos, C. F. Costa, W. R. Scarano, R. M. Góes, S. R. Taboga, Key participants of the tumor microenvironment of the prostate: an approach of the structural dynamic of cellular elements and extracellular matrix components during epithelial-stromal transition, *Acta Histochem,* Vol. 117, No. 1, pp. 4-13, Jan, 2015. eng

[57] M. P. Caley, H. King, N. Shah, K. Wang, M. Rodriguez-Teja, J. H. Gronau, J. Waxman, J. Sturge, Tumor-associated Endo180 requires stromal-derived LOX to promote metastatic prostate cancer cell migration on human ECM surfaces, *Clin Exp Metastasis,* Vol. 33, No. 2, pp. 151-65, Feb, 2016. eng

[58] Z. Liu, L. Wang, H. Xu, Q. Du, L. Li, L. Wang, E. S. Zhang, G. Chen, Y. Wang, Heterogeneous Responses to Mechanical Force of Prostate Cancer Cells Inducing Different Metastasis Patterns, *Adv Sci (Weinh),* Vol. 7, No. 15, pp. 1903583, Aug, 2020. eng

[59] K. M. Aw Yong, Y. Sun, S. D. Merajver, J. Fu, Mechanotransduction-Induced Reversible Phenotypic Switching in Prostate Cancer Cells, *Biophys J,* Vol. 112, No. 6, pp. 1236-1245, Mar 28, 2017. eng

[60] J. L. Eisenberg, A. Safi, X. Wei, H. D. Espinosa, G. S. Budinger, D. Takawira, S. B. Hopkinson, J. C. Jones, Substrate stiffness regulates extracellular matrix deposition by alveolar epithelial cells, *Res Rep Biol,* Vol. 2011, No. 2, pp. 1-12, Jan, 2011. eng

[61] A. Petersen, P. Joly, C. Bergmann, G. Korus, G. N. Duda, The impact of substrate stiffness and mechanical loading on fibroblast-induced scaffold remodeling, *Tissue Eng Part A,* Vol. 18, No. 17-18, pp. 1804-17, Sep, 2012. eng

[62] O. V. Sazonova, K. L. Lee, B. C. Isenberg, C. B. Rich, M. A. Nugent, J. Y. Wong, Cell-cell interactions mediate the response of vascular smooth muscle cells to substrate stiffness, *Biophys J,* Vol. 101, No. 3, pp. 622-30, Aug 3, 2011. eng

[63] Z. Goli-Malekabadi, M. Tafazzoli-Shadpour, A. Tamayol, E. Seyedjafari, Time dependency of morphological remodeling of endothelial cells in response to substrate stiffness, *Bioimpacts,* Vol. 7, No. 1, pp. 41-47, 2017. eng

[64] X. Tang, Y. Zhang, J. Mao, Y. Wang, Z. Zhang, Z. Wang, H. Yang, Effects of substrate stiffness on the viscoelasticity and migration of prostate cancer cells examined by atomic force microscopy, *Beilstein Journal of Nanotechnology,* Vol. 13, pp. 560-569, //, 2022.

[65] A. J. McKenzie, S. R. Hicks, K. V. Svec, H. Naughton, Z. L. Edmunds, A. K. Howe, The mechanical microenvironment regulates ovarian cancer cell morphology, migration, and spheroid disaggregation, *Scientific Reports,* Vol. 8, No. 1, pp. 7228, 2018/05/08, 2018.

[66] Y. Fan, Q. Sun, X. Li, J. Feng, Z. Ao, X. Li, J. Wang, Substrate Stiffness Modulates the Growth, Phenotype, and Chemoresistance of Ovarian Cancer Cells, *Frontiers in Cell and Developmental Biology,* Vol. 9, 2021-August-24, 2021. English

[67] L. Chen, G. Zhao, M. De Menna, S. Coppola, N. Landman, S. Schieven, A. Groenewoud, G. N. Thalmann, T. Schmidt, J. de Vries, Mechano-signaling of prostate tumor initiating cells facilitates their tropism to stiff metastatic niche, *bioRxiv*, pp. 2023.08. 28.553410, 2023.

[68] V. Gkretsi, T. Stylianopoulos, Cell adhesion and matrix stiffness: coordinating cancer cell invasion and metastasis, *Frontiers in oncology,* Vol. 8, pp. 145, 2018.

[69] L. E. Lamb, J. C. Zarif, C. K. Miranti, The androgen receptor induces integrin α6β1 to promote prostate tumor cell survival via NF-κB and Bcl-xL Independently of PI3K signaling, *Cancer research,* Vol. 71, No. 7, pp. 2739-2749, 2011.

[70] R. Ata, C. N. Antonescu, Integrins and cell metabolism: an intimate relationship impacting cancer, *International journal of molecular sciences,* Vol. 18, No. 1, pp. 189, 2017.

[71] A. K. Simi, M.-F. Pang, C. M. Nelson, Extracellular matrix stiffness exists in a feedback loop that drives tumor progression, *Biomechanics in Oncology*, pp. 57-67, 2018.

[72] A. N. Gargalionis, K. A. Papavassiliou, A. G. Papavassiliou, Targeting the YAP/TAZ mechanotransducers in solid tumour therapeutics, *Journal of Cellular and Molecular Medicine,* Vol. 27, No. 13, pp. 1911, 2023.

[73] S. A. Mosaddad, Y. Salari, S. Amookhteh, R. S. Soufdoost, A. Seifalian, S. Bonakdar, F. Safaeinejad, M. M. Moghaddam, H. Tebyanian, Response to mechanical cues by interplay of YAP/TAZ transcription factors and key mechanical checkpoints of the cell: a comprehensive review, *Cell Physiol Biochem,* Vol. 55, No. 1, pp. 33-60, 2021.

[74] G. Rubí-Sans, A. Nyga, M. A. Mateos-Timoneda, E. Engel, Substrate stiffness-dependent activation of Hippo pathway in cancer associated fibroblasts, *Biomaterials Advances,* Vol. 166, pp. 214061, 2025.

[75] C. W. Molter, E. F. Muszynski, Y. Tao, T. Trivedi, A. Clouvel, A. J. Ehrlicher, Prostate cancer cells of increasing metastatic potential exhibit diverse contractile forces, cell stiffness, and motility in a microenvironment stiffness-dependent manner, *Frontiers in Cell and Developmental Biology,* Vol. 10, pp. 932510, 2022.

[76] H. Y. Murad, H. Yu, D. Luo, E. P. Bortz, G. M. Halliburton, A. B. Sholl, D. B. Khismatullin, Mechanochemical disruption suppresses metastatic phenotype and pushes prostate cancer cells toward apoptosis, *Molecular Cancer Research,* Vol. 17, No. 5, pp. 1087-1101, 2019.

[77] W. Pan, Z. Zhang, H. Kimball, F. Qu, K. Berlind, K. H. Stopsack, G.-S. M. Lee, T. K. Choueiri, P. W. Kantoff, Abiraterone acetate induces CREB1 phosphorylation and enhances the function of the CBP-p300 complex, leading to resistance in prostate cancer cells, *Clinical Cancer Research,* Vol. 27, No. 7, pp. 2087-2099, 2021.

[78] M. P. Edlind, A. C. Hsieh, PI3K-AKT-mTOR signaling in prostate cancer progression and androgen deprivation therapy resistance, *Asian journal of andrology,* Vol. 16, No. 3, pp. 378-386, 2014.

[79] J. B. Wu, L. W. Chung, The PI3K-mTOR Pathway in Prostate Cancer: Biological Significance and Therapeutic Opportunities, *PI3K-mTOR in Cancer and Cancer Therapy*, pp. 263-289, 2016.

[80] R. Wang, Z. Qu, Y. Lv, L. Yao, Y. Qian, X. Zhang, L. Xiang, Important Roles of PI3K/AKT Signaling Pathway and Relevant Inhibitors in Prostate Cancer Progression, *Cancer Medicine,* Vol. 13, No. 21, pp. e70354, 2024.

[81] S. Heller, T. Sugawara, E. Nevedomskaya, S. J. Baumgart, H. Nguyen, E. Corey, A. Böhme, O. von Ahsen, O. Politz, B. Haendler, Abstract B065: Combining the androgen receptor inhibitor darolutamide with PI3K/AKT/mTOR pathway inhibitors has superior efficacy in preclinical models of prostate cancer, *Cancer Research,* Vol. 83, No. 11_Supplement, pp. B065-B065, 2023.

[82] S. Li, F. La Manna, P. Chouvardas, G. Thalmann, M. Kruithof-de Julio, Abstract B007: New generation mTOR blocker sensitizes prostate cancer models to AR-targeting therapy, *Cancer Research,* Vol. 83, No. 11_Supplement, pp. B007-B007, 2023.